ChemComm

COMMUNICATION

View Article Online
View Journal | View Issue

Cite this: *Chem. Commun.*, 2014, **50**, 9903

Received 24th April 2014,
Accepted 30th June 2014

DOI: 10.1039/c4cc03059a

www.rsc.org/chemcomm

Modulated SmA_b phases formed by anchor shaped liquid crystalline molecules†

Karina Geese, Marko Prehm and Carsten Tschierske*

Bent-core molecules with a linear alkyl chain in the bay position (anchor shaped molecules) form new liquid crystalline phases combining periodicities with different coherence lengths in distinct directions; in these LC phases the molecules are organized on average orthogonal in modulated layers (ribbons or patches) with restricted rotation around the long axis, thus representing modulated SmA_b phases.

Liquid crystals (LCs) represent spatially ordered dynamic systems which self-assemble into minimum energy and maximum entropy state soft or fluid superstructures.[1] These are of contemporary interest for numerous applications, such as displays, optical modulators, biosensors and as tools for the regular spatial organization of nanoparticles and organic semiconductors.[2] Order can occur in at least one and up to three directions and is divided into orientational and positional order. Orientational order mainly results from parallel alignment of anisometric units, whereas positional order is often the result of the segregation of incompatible segments of the molecules. This combination of order and dynamics is often achieved by the combination of anisometric rigid segments providing orientational order with flexible units providing the required mobility. Thereby, the molecular shape, the mode of connection of rigid and flexible units and the degree of incompatibility between them are of significant importance. If flexible chains are grafted exclusively to the ends of rod-like anisometric molecules (Fig. 1a), then lamellar phases (smectic phases = Sm) are dominating. Identical chains in terminal and lateral positions at rod-like cores cause a loss of positional order, mainly providing nematic phases (N) involving only orientational order.[3] The loss of positional order could be avoided by using incompatible lateral and terminal chains. In this case a variety of complex LC phase structures, mostly representing columnar phases with polygonal honeycomb structures and different (triangular, square, pentagonal, hexagonal…) shapes (Col) has been reported.[1,4] For molecules with a bent aromatic core (Fig. 1b) the combination of incompatible end- and side-chains restricts the shape of these cylinders to hexagonal (Col_{hex}),[5] whereas compounds without lateral chain, well known as bent-core mesogens, provide ferroelectric and antiferroelectric switching polar smectic phases (SmP).[6] Though there are some few previous reports about bent-core mesogens with additional lateral alkyl chains, these were attached either to the convex outer side of the bent core (bell-shaped molecules),[7] or to the peripheral rod-like wings,[8,9] which both lead to a suppression of the positional order, predominately generating isotropic liquids and nematic phases.

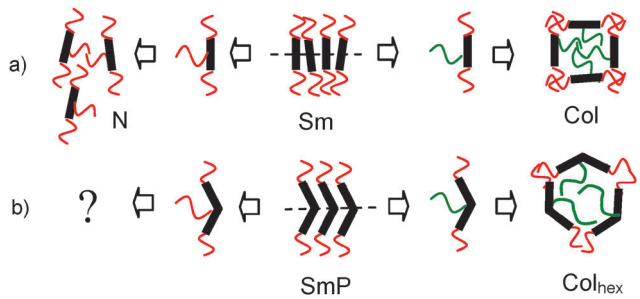

Fig. 1 Self-assembly of (a) rod-like and (b) bent-core molecules with or without additional lateral chains; the lateral chains (red) can be identical with the terminal chains (red) or different and incompatible with them (green).

Herein we report a new class of anchor-shaped mesogens, comprising a bent rigid core unit involving in total 7 aromatic rings, combined with two alkyl end-chains and an additional long lateral *n*-alkyl chain at the convex side, in the inner bay-position of the bent aromatic core (see Fig. 1b, left and formula in Table 1). This kind of compounds provides access to a series of new LC phase structures representing biaxial SmA phases (SmA_b phases[10–13]) with additional modulations in two or three dimensions and combining different coherence lengths in the distinct directions.

The synthesis of the compounds **1/*n***, **1F/22** and **2/22** is shown in Scheme 1. It starts with 2′-alkoxy-*m*-terphenyl-4,4″-diols **4/*n***

Institute of Chemistry, Organic Chemistry, Martin-Luther University Halle-Wittenberg, Kurt-Mothes Str. 2, 06120 Halle, Germany. E-mail: carsten.tschierske@chemie.uni-halle.de; Fax: +49 345 5525664; Tel: +49 345 5527346

† Electronic supplementary information (ESI) available: Synthesis, analytical data, DSC traces, additional XRD patterns, textures and other data. See DOI: 10.1039/c4cc03059a

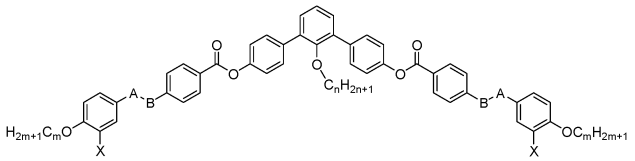

Table 1 Phase transition of compounds **1/*n***, **1F/22** and **2/22**[a]

Comp.	X	A–B	*m*	*n*	*T*/°C [Δ*H*/kJ mol^{-1}]
1/6	H	COO	8	6	Cr 149 [27.5] $SmÃ_b^{\#}$ 155 [15.0] Iso
1/18	H	COO	8	18	Cr 132 [60.2] ($SmÃ_b$/*c2mm*$^{\#}$ 127 [15.4]) Iso
1F/22	F	COO	8	22	Cr 122 [52.2] (Col_{rec}/*c2mm*$^{\#}$ 111 [0.1]) $SmÃ_b$/*c2mm*$^{\#}$ 126 [19.4] Iso
2/22	H	—	6	22	Cr 145 [64.7] $SmÃ_b$/*c2mm*$^{\#}$ 147 [21.4] Iso

[a] Transition temperatures and corresponding enthalpy values were determined by DSC (first heating, 10 K min^{-1}, peak temperatures); monotropic transitions (in parenthesis) were determined on cooling; abbreviations: $SmÃ_b^{\#}$ = biaxial SmA phase formed by intercalated ribbons with short range correlation; $SmÃ_b$/*c2mm*$^{\#}$ = modulated, smectic phase with short range rectangular *c2mm* lattice; Col_{rec}/*c2mm*$^{\#}$ = rectangular columnar mesophase with long range *c2mm* lattice. $^{\#}$ indicates the presence of an additional short range electron density modulation. For DSC traces, textures and crystallographic data see Fig. S1–S8 and Table S1 (ESI).

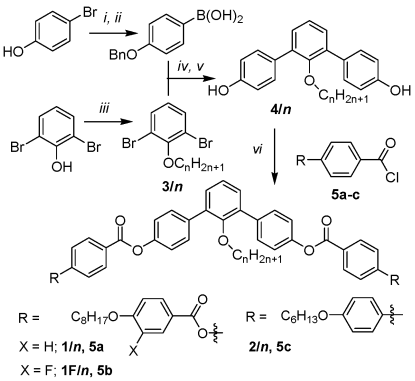

Scheme 1 Synthesis of the compounds; reagents and conditions: (i) BnCl, K_2CO_3, 2-butanone, reflux, 5 h; (ii) (1) *n*-BuLi, THF, −80 °C, 1 h, (2) $B(OMe)_3$, THF, −80 °C, over night to RT, (3) HCl, RT, 1 h; (iii) $H_{2m+1}C_mBr$, K_2CO_3, MeCN, reflux, 12 h; (iv) $Pd(PPh_3)_4$, Na_2CO_3 (aq.), THF, reflux, 12 h; (v) H_2, Pd/C, THF, 24 h; (vi) pyridine, Et_3N, CH_2Cl_2, reflux, 4 h.†

which were obtained from the 2-alkoxy-1,3-dibromobezenes **3/*n*** by Suzuki reaction[14] with 4-benzyloxybenzene boronic acid.[15,16] followed by cleavage of the benzylic ethers with H_2, Pd/C.[17] Esterification of the bent *m*-terphenyl diols **4/*n*** with appropriately 4-substituted benzoyl chlorides **5a–c** results in the desired bent-core molecules which were purified by column chromatography and repeated crystallization (for details see ESI†).

The transition temperatures and associated transition enthalpies are summarized in Table 1. All investigated compounds form liquid crystalline phases which appear with typical fan-shaped textures (see Fig. 2a) indicating smectic phases. The dark extinction crosses are parallel to the directions of polarizer and analyzer (see Fig. 2a; Fig. S5a, S6 and S7a, ESI†) in all LC phases, indicating either on average non-tilted (SmA) or anticlinic tilted smectic phases (SmC_a). Shearing of the samples leads to birefringent Schlieren textures,

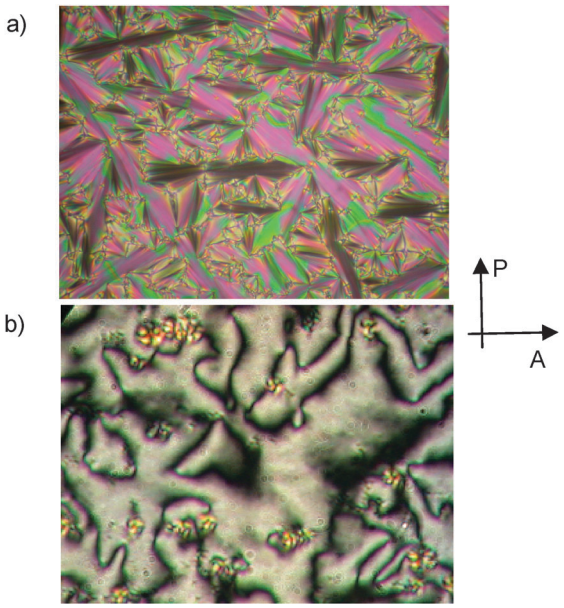

Fig. 2 Textures of the $SmÃ_b$/*c2mm*$^{\#}$ phase of **1/18** as observed between crossed polarizers, (a) fan-shaped texture at 120 °C (planar alignment) and (b) texture of the sheared sample at 124 °C (homeotropic alignment, the birefringent spots are areas where realignment back to the planar texture starts. The textures of compounds **1/6**, **1F/22** and **2/22** are shown in Fig. S5–S7†).

which confirm the optical biaxiality of these smectic phases (see Fig. 2b and Fig. S7b, ESI†). Only two brush disclinations can be observed (defects of the strength $S = \pm 1/2$, two dark brushes meet at the disclination points). The absence of 4-brush disclinations in the Schlieren textures is typical for non-tilted biaxial SmA_b phases (Mc Millan phases),[10] where the hindered rotation of the molecules around the long axis and not a uniform molecular tilt leads to optical biaxiality.[11–13] The non-tilted organization of the molecules is further corroborated by X-ray diffraction (XRD) of aligned samples, where the diffuse wide angle scattering, located on the equator (d = 0.46–0.47 nm) and corresponding to the mean lateral distance between the molecules has its maxima perpendicular to the sharp layer reflection occurring in the small angle region on the meridian (Fig. 3a–d).

For compound **1/6** with the shortest lateral chain (Fig. 3a) the layer distance is d_1 = 2.75 nm (T = 150 °C) and increases slightly with decreasing temperature (d_1 = 2.79 nm at 120 °C). So, the layer distance conforms roughly to half of the molecular length (L_{mol} = 5.7 nm). Consequently, the smectic phase can be considered as an intercalated SmA_b phase. There is an additional very weak diffuse scattering positioned in the small angle region on the equator with its maximum at d_2 = 1.5 nm (arrows in Fig. 3a). This diffuse small angle scattering is perpendicular to the layer reflection and indicates a short range in-plane periodicity with an estimated coherence length of about ~4 nm (see Fig. S9 and Table S2†). The intensity and the mean distance d_2 of this scattering increase with growing length of the lateral chain (Fig. 3a and b, Table 2), suggesting that it is caused by the segregation of the lateral alkyl chains from the aromatic cores. The LC phases showing this additional small angle scattering are indicated by the superscript$^{\#}$ in the phase assignment code.

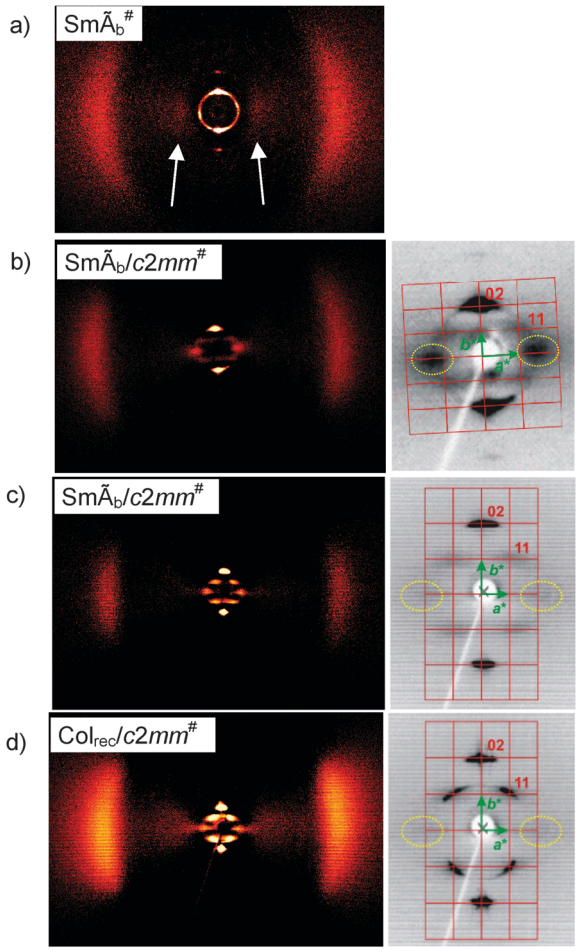

Fig. 3 XRD pattern of a surface aligned sample of the mesophases of compounds (a) **1/6** at T = 120 °C, (b) **1/18** at T = 150 °C, (c) **1F/22** in the $SmÃ_b/c2mm^{\#}$ phase at 123 °C and (d) in the $Col_{rec}/c2mm^{\#}$ phase at 110 °C; at the left complete patterns and at the right small angle regions with reciprocal lattice, see also Table S1 for crystallographic data.†

The LC phase of **1/6** is designated as $SmÃ_b^{\#}$, a modulated SmA_b phase with short range 2D-lattice and additional short range periodicity perpendicular to this modulation, as explained below in more detail.

The XRD pattern of the surface aligned sample of compound **1/18** (Fig. 3b) shows a similar pattern as **1/6**, but with a higher intensity of the diffuse small angle scatterings on the equator (coherence length ~11 nm). Moreover, there are four additional weak and diffuse cross reflections outside of meridian and equator. The layer reflections on the meridian and the diffuse cross reflections were indexed as 20, respectively 11 reflection of a rectangular lattice (a = 3.84, b = 5.17 nm at T = 125 °C) with *c2mm* symmetry and limited coherence length (Fig. 3b, right). The diffuse scattering maximum on the equator is shifted to d_2 = 2.5 nm. The diffraction patterns of compounds **1F/22** with additional peripheral F-substituents and compound **2/22** with biphenyl wings instead of the phenyl benzoate wings (Fig. S8†) are similar to **1/18** (Fig. 3c, see also Table 2). Because the coherence length of the 2D lattice is much smaller than that of the layer periodicity theses phases are assigned as modulated smectic phases ($SmÃ_b/c2mm^{\#}$).

Table 2 XRD parameters of compounds **1/*n***, **1F/22** and **2/22**[a]

Comp.	Phase (T/°C)	d_1/nm	a/nm	b/nm	d_2/nm
1/6	$SmÃ_b^{\#}$ (120)	2.79			1.5
1/18	$SmÃ_b/c2mm^{\#}$ (125)		3.84	5.17	2.5
1F/22	$SmÃ_b/c2mm^{\#}$ (123)		5.54	5.07	3.2
1F/22	$Col_{rec}/c2mm^{\#}$ (110)		5.75	5.07	3.2
2/22	$SmÃ_b/c2mm^{\#}$ (145)		6.32	4.48	2.8

[a] For XRD patterns, see Fig. 3 and Fig. S8 (ESI).

For the fluorinated compound **1F/22** an additional phase transition with a small enthalpy takes place at T = 111 °C (Table 1, for DSC traces, see Fig. S3†) without visible change of the texture (see Fig. S6†), retaining a typical fan-like appearance, similar to that shown in Fig. 2a. However, this transition is associated with a clear change of the XRD pattern (Fig. 3c and d). The XRD pattern of the high temperature mesophase (T = 123 °C, Fig. 3c) is similar to the patterns observed for the non-fluorinated compound **1/18** (Fig. 3b). At the phase transition to the low temperature phase all reflexions remain on their positions. However, the diffuse 11 reflections turn to sharp Bragg peaks while the scatterings on the equator do not change (Fig. 3d). Thus, the 2D lattice becomes long range, and therefore, this phase is assigned as a columnar phase ($Col_{rec}/c2mm^{\#}$). The diffuse scatterings on the equator, which are incommensurate to the 2D lattice, indicate an additional short range periodicity (d_2) perpendicular to the *c2mm* lattice. This is most probably due to an electron density modulation along the ribbons. In this $Col_{rec}/c2mm^{\#}$ phase there is no correlation between the 2D lattice and the short range modulation. Therefore, this phase does not represent a true 3D mesophase, but a 2D structure with an additional electron density modulation in the third direction of space.‡

A model of this low temperature phase is shown in Fig. 4d. The same model of organization, but with shorter correlation lengths of parameter a can also be assumed for the local structures in the less ordered $SmÃ_b/c2mm^{\#}$ and $SmÃ_b^{\#}$ phases.

The development of the different phase types can be understood in the following way. Bent-core mesogens usually organize in layers with separated cores and end-chains. However, the lateral alkyl chains increase the effective cross sectional area of the core units and this leads to a layer frustration, giving rise to a layer modulation, *i.e.* a disruption of the layers into ribbons. These ribbons have a tendency for staggered packing, due to the favourable mixing of some lateral with the terminal alkyl chains (see Fig. 4b). This retains positional order (suppresses formation of isotropic liquids or nematic phases) and favours a packing of these ribbons on a centred rectangular lattice (*c2mm*), leading to intercalated smectic phases with local *c2mm* lattice. For **1/6** with the shortest chain there is only short range correlation of these ribbons along direction a, which does not give rise to a detectable scattering. Therefore, this LC phase is considered as an intercalated biaxial smectic phase ($SmÃ_b^{\#}$). This is a new type of non-polar SmA_b phases, distinct from the previously reported monolayer[11,12] and bilayer types[13] with some similarity to the so-called B_6 phases formed by bent-core molecules.§[18] The feature in common with the B_6 phases is the presence of a short range layer modulation which is indicated by a tilde (~) in the phase assignment used here.

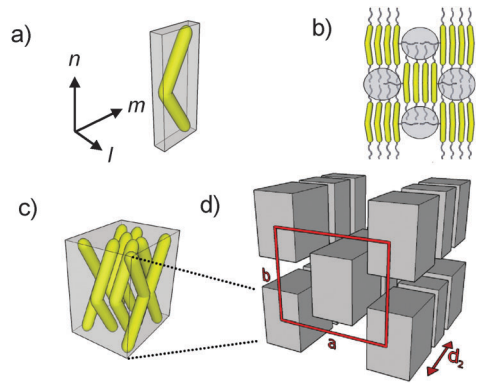

Fig. 4 Models showing the proposed organization of the molecules in the distinct $SmA_b^{\#}$ phases: (a) frozen rotation of the molecules around the long axis, leading to biaxiality; (b) mixing of terminal and lateral chains stabilizes the staggered packing on the *c2mm* lattice; (c) biaxial organization of the molecules in the batches; (d) stacking of the batches in ribbons and organization of the ribbons on a *c2mm* lattice leads to the $Sm\tilde{A}_b/c2mm^{\#}$ and $Col_{rec}/c2mm^{\#}$ phases; the space between the batches is filled by the terminal and the lateral alkyl chains; the periodicity d_2 has only short coherence length in all phases.

In the $Sm\tilde{A}_b/c2mm^{\#}$ phases of the long chain compounds the correlation length of the *c2mm* lattice is increased, thus providing the additional diffuse 11 scatterings. As shown in Table 2, with rising length of the lateral chain the parameters a (related to the diameter of the ribbons) as well as d_2 (modulation along the ribbons) increase, whereas the parameter b remains nearly constant and is exclusively determined by the molecular length L_{mol} ($b \sim L_{mol}/2$). At reduced temperature this *c2mm* lattice could become long range, as in the $Col_{rec}/c2mm^{\#}$ phase of compound **1F/22**.

As indicated in Fig. 4d the short range periodicity d_2 results from a modulation of the ribbons which is most likely caused by a fracturing of the ribbons into strings of patches with enhanced concentration of the aromatic cores (Fig. 4c and d). The reason is that the lateral alkyl chains segregate from the aromatic cores, thus providing a periodicity with short coherence length along the ribbon long axis. These patches have an average size of ~12 and ~22 molecules for **1/18** and **1F/22**, respectively (for calculations, see Table S3†). It is hypothesized that in the patches the rotation of the molecules around their long axes is restricted, leading to biaxiality but no long range polar order is achieved,¶ as the lateral chains distort a polar packing. In analogy to the organization in B_6 and B_{1Rev} phases of bent-core mesogens without lateral chains,[6,18,19a] a preferred alignment of the biaxial vector ***m*** parallel to the ribbon long axis is considered (Fig. 4a and b). This mode of packing should be favoured as it allows easy fluctuations along the ribbons with retention of a dense packing, thus providing an entropy gain. These fluctuations are thought to distort the formation of a long range molecular register along the ribbons, retaining the diffuse character of d_2 in all LC phases. It is interesting to note that despite of the presence of positional order in more than only one direction, all these LC phases appear optically like simple biaxial smectic A phases, characterized by fan-like and Schlieren textures (see Fig. 2 and Fig. S5–S7†).

Overall, introduction and elongation of a lateral chain in the bay position of bent-core mesogens has significant influence on their self-assembly, giving rise to new LC phase structures. Tilted and polar smectic phases are removed, but biaxial order is retained, thus providing a new way to non-polar SmA_b phases. These SmA_b phases are additionally modulated, thus giving rise to unique modes of LC self-assembly, leading to increased structural complexity in these self-assembled soft matter systems.

This work was supported by the EU within the FP7 funded Collaborative project BIND (grant No. 216025).

Notes and references

‡ Though there are numerous 2D modulated LC phases of bent-core mesogens, to the best of our knowledge there is presently only one report about a long range 3D modulated LC structure formed by bent-core molecules.[19b] However in the reported cases there is long range periodicity in all three dimensions, whereas in our case there is reduced coherence length in at least one of the direction.

§ There are also clear differences to the known B_6-type intercalated smectic phases. The formation of a Schlieren texture upon shearing is usually not observed for B_6 phases. Moreover, though in B_6 phases a diffuse XRD scattering can sometimes be observed as 11 scatterings between equator and meridian, a diffuse small angle scattering was never observed on the equator.[18]

¶ The effect of a triangular wave electric field on the mesophases was investigated for compounds **1/6** and **1F/22** as representatives. No polar switching could be detected under an applied field up to 60 V μm^{-1}, and therefore, there should be no macroscopic polar order in these LC phases.

1 C. Tschierske, *Angew. Chem., Int. Ed.*, 2013, **52**, 8828.
2 *Handbook of Liquid Crystals*, ed. J. W. Goodby, P. J. Collings, T. Kato, C. Tschierske, H. F. Gleeson and P. Raynes, Wiley-VCH, Weinheim, 2nd edn, 2014.
3 W. Weissflog and D. Demus, *Cryst. Res. Technol.*, 1984, **19**, 55.
4 C. Tschierske, C. Nürnberger, H. Ebert, B. Glettner, M. Prehm, F. Liu, X.-B. Zeng and G. Ungar, *Interface Focus*, 2012, **2**, 669.
5 B. Glettner, F. Liu, X. Zeng, M. Prehm, U. Baumeister, G. Ungar and C. Tschierske, *Angew. Chem., Int. Ed.*, 2008, **47**, 6080.
6 R. A. Reddy and C. Tschierske, *J. Mater. Chem.*, 2006, **16**, 907; H. Takezoe and Y. Takanishi, *Jpn. J. Appl. Phys.*, 2006, **45**, 597; A. Eremin and A. Jakli, *Soft Matter*, 2013, **9**, 615.
7 J. Matraszek, J. Mieczkowski, J. Szydlowska and E. Gorecka, *Liq. Cryst.*, 2000, **27**, 429; N. Vaupotic, J. Szydlowska, M. Salamonczyk, A. Kovarova, J. Svoboda, M. Osipov, D. Pociecha and E. Gorecka, *Phys. Rev. E: Stat. Phys., Plasmas, Fluids, Relat. Interdiscip. Top.*, 2009, **80**, 030701; D. Z. Obadovic, A. Vajda, A. Jakli, A. Menyhard, M. Kohout, J. Svoboda, M. Stojanovic, N. Eber, G. Galli and K. Fodor-Csorba, *Liq. Cryst.*, 2010, **37**, 527; M. V. Srinivasan and P. Kannan, *J. Mater. Sci.*, 2011, **46**, 5029.
8 J. Seltmann and M. Lehmann, *Liq. Cryst.*, 2011, **38**, 407.
9 W. Weissflog and U. Baumeister, *Liq. Cryst.*, 2013, **40**, 959.
10 H. R. Brand, P. E. Gladis and H. Pleiner, *Macromolecules*, 1992, **25**, 7223.
11 H. F. Leube and H. Finkelmann, *Makromol. Chem.*, 1991, **192**, 1317; T. Hegmann, J. Kain, S. Diele, G. Pelzl and C. Tschierske, *Angew. Chem., Int. Ed.*, 2001, **40**, 887.
12 K. Kishikawa, T. Inoue, Y. Sasaki, S. Aikyo, M. Takahashi and S. Kohmoto, *Soft Matter*, 2011, **7**, 7532.
13 B. K. Sadashiva, R. Amaranatha Reddy, R. Pratibha and N. V. Madhusudana, *J. Mater. Chem.*, 2002, **12**, 943; R. Pratibha, N. V. Madhusudana and B. K. Sadashiva, *Science*, 2000, **288**, 2184; C. V. Yelamaggad, I. S. Shaahikala, V. P. Tamilenthi, D. S. Shanker Rao, G. G. Nair and S. K. Prasad, *J. Mater. Chem.*, 2008, **18**, 2096.
14 N. Miyaura, T. Yanagi and A. Suzuki, *Synth. Commun.*, 1981, **11**, 513–519.
15 V. Percec and G. Johansson, *J. Mater. Chem.*, 1993, **3**, 83.
16 M. Hird, G. W. Gray and K. J. Toyne, *Mol. Cryst. Liq. Cryst.*, 1991, **206**, 187.
17 C. H. Heathcock and R. Ratcliffe, *J. Am. Chem. Soc.*, 1971, **93**, 1746.
18 S. Kang, M. Tokita, Y. Takanishi, H. Takezoe and J. Watanabe, *Phys. Rev. E: Stat. Phys., Plasmas, Fluids, Relat. Interdiscip. Top.*, 2007, **78**, 042701; S. Kang, S. K. Lee, M. Tokita and J. Watanabe, *Phys. Rev. E: Stat. Phys., Plasmas, Fluids, Relat. Interdiscip. Top.*, 2009, **80**, 042703.
19 (*a*) N. Vaupotic, D. Pociecha and E. Gorecka, *Top. Curr. Chem.*, 2012, **318**, 281; (*b*) J. Szydlowska, J. Mieczkowski, J. Matraszek, D. W. Bruce, E. Gorecka, D. Pociecha and D. Guillon, *Phys. Rev. E: Stat. Phys., Plasmas, Fluids, Relat. Interdiscip. Top.*, 2003, **67**, 031702.

